

**MODELING CREEP RATCHETING OF AN ALUMINUM-SILICON
 EUTECTIC ALLOY**

H. Altenbach¹

Martin-Luther-University
 Halle-Wittenberg
 Halle, Germany

S. Kozhar

Otto-von-Guericke-
 University Magdeburg
 Magdeburg, Germany

K. Naumenko

Martin-Luther-University
 Halle-Wittenberg
 Halle, Germany

ABSTRACT

Eutectic AlSi12CuNiMg cast alloy combines excellent mechanical properties with good castability and is commonly used for piston applications. Creep responses of this alloy under constant and cyclic force at elevated temperatures of 250°C and 300°C are presented. In addition, the alloy is studied in both P-refined and Sr-modified conditions at temperature of 300°C. The T6 heat treatment is used to affect the microstructure and hardness. Based on experimental data correlations between the microstructure and the force-controlled low-cycle fatigue are found. The fracture surfaces of the specimens are investigated with the help of the optical and scanning electron microscopy.

For the description of the material behavior a unified model of viscoplasticity is suggested. The primary and secondary stages of experimental curves are modeled with the help of a non-linear kinematic hardening rule and the classical creep functions of stress. To describe the final part of the tertiary creep stage, the damage variable has to be applied.

INTRODUCTION

The eutectic aluminium alloy AlSi12CuNiMg investigated in the present work is widely used for load-bearing structural components in the automotive industry. The most important areas of application for the alloy are pistons for combustion engines, gears, pump parts, wear-resistant and heat-resistant parts of all kinds owing to its high strength at elevated temperatures and low thermal expansion coefficient. Nevertheless, to apply these alloys successfully in highly loaded components, it is essential to understand their strength properties under various loading conditions [1, 2].

The goal of the present study is to:

- describe the alloy behavior under applied static and cyclic loading at an elevated temperature in P-refined condition;
- examine the effect of the microstructure on the low cycle fatigue strength at 300°C in both P-refined and Sr-modified condition.

Table 1 Chemical composition of the studied alloys (wt.%)

Alloy code	Si	Cu	Ni	Mg	Mn	Fe	Ti	P	Sr	other	Al
M-F	12.65	1.11	0.81	0.99	0.20	0.28	0.05	<0.001	0.025	<0.01	rem.
R-T6	12.72	1.07	0.95	1.12	0.16	0.41	0.05	0.005	<0.0005	<0.01	rem.
M-T6	12.44	1.14	0.88	0.99	0.19	0.24	0.04	<0.001	0.027	<0.01	rem.

¹ Corresponding author. Email holm.altenbach@iw.uni-halle.de (Prof. Dr.-Ing. Holm Altenbach)

1. EXPERIMENTAL PROCEDURE

The cast aluminum alloy AlSi12CuNiMg was used in three conditions: P-refined and heat-treated (hereafter termed alloy R-T6), Sr-modified in the as-cast state (M-F), and Sr-modified after T6 heat treatment (M-T6). The chemical composition of the alloys is shown in Table 1. P-refined and Sr-modified samples were heat-treated under T6 conditions, i.e. solution treated at 510°C for 6 h in an air circulate furnace, water quenched at 50°C, naturally aged at room temperature for 24 h, and then artificially aged at 165°C for 8 h. Microstructural changes were examined using optical and scanning electron microscopy.

Tensile testing of specimens was carried out at room temperature and at 300°C in a Zwick Z250 testing machine in accordance with the DIN EN 10002 procedure. Three tensile tests were carried out for each alloy and temperature value. The test specimens were held during 15 min at 300°C before mechanical testing. The hardness of the as-cast and heat-treated specimens was measured at room temperature with a Brinell hardness tester with a load of 62.5 kg and a ball diameter of 2.5 mm.

Specimens for creep and cyclic testing with a diameter of 5 mm, length of 120 mm and gauge length of 50 mm were machined from the ingots. The surfaces of the specimens were polished. Tests were performed on a servohydraulic fatigue testing machine MTS-810 with 250 kN maximum load. To measure the strain, an extensometer with a gauge length of 12.5 mm was applied. The specimens were heated with a 5 kW induction heater. The thermal strain was subtracted from the total strain.

Force-controlled fatigue tests were conducted at an elevated temperature in laboratory air under low cycle fatigue conditions. The minimum to maximum stress ratio was kept at 0. This means that the cycling was fulfilled in the pure tensile state without a stress reversal, i.e. cyclic creep or ratcheting condition. Later on some of the broken specimens were observed with the help of light microscopy and scanning electron microscopy to determine the damage mechanisms.

The loading conditions for given alloys are summarized in Table 2.

Table 2 Fulfilled experiments

Alloy code	Tensile test	Creep test	Cyclic test ($R_\sigma = 0$)
M-F	T = 20, 300°C	—	T = 300°C f = 0.1 Hz
R-T6	T = 20, 250, 300°C	T = 250, 300°C	T = 250, 300°C f = 0.1, 1 Hz
M-T6	T = 20, 300°C	—	T = 300°C f = 0.1 Hz

2. EXPERIMENTAL RESULTS

The microstructure of the investigated alloys is presented in Fig. 1. For both M-F and M-T6 alloys the addition of strontium causes a complete elimination of primary silicon crystals. However, the specimens with the modified structures contain spherical pores that can be explained by contamination with hydrogen during the addition of strontium. The porosity value obtained for strontium modified alloys M-F and M-T6 is 2.6%. In contrast to that the porosity value for alloy R-T6 is only 0.5%. The modified eutectic silicon fibers, regions of dendritic aluminum and intermetallics can be seen in the microstructure of the modified alloy M-F in the as-cast condition (Fig. 1a). Addition of phosphorus has led to the refinement of the primary silicon crystals in the alloy R-T6. The aluminum matrix of this alloy R-T6 contains primary silicon as well as eutectic acicular silicon and numerous intermetallics (Fig. 1b).

The effect of T6 heat-treatment for both the refined R-T6 and modified M-T6 alloys leads to essential changes in their structures and properties. After tempering of the refined R-T6 alloy, the primary silicon crystals and eutectic silicon needles show only some spheroidizing. The modified and heat-treated alloy M-T6 shows distinctly more uniform and refined structures due to the combined effects of modification and T6 heat treatment (Fig. 2), i.e., the eutectic silicon is rounded and creates a partially broken eutectic network.

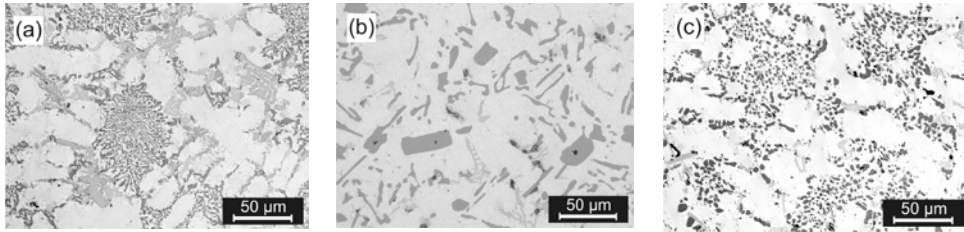


Fig. 1 Microstructure of M-F alloy (a), R-T6 alloy (b) and M-T6 alloy (c). Light microscope observation with magnification of 500

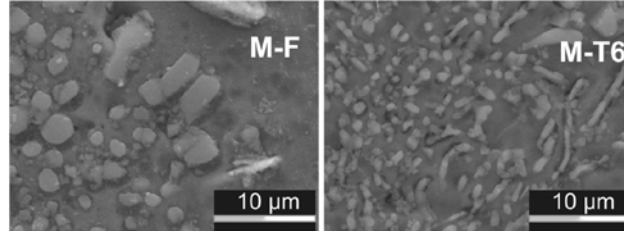


Fig. 2 SEM micrographs of the Sr-modified M-F and M-T6 alloys

Table 3 presents the average tensile properties of investigated alloys at 20°C and 300°C. It is apparent that the heat treatment can be highly beneficial for alloys performance. The highest ductility is found in the modified alloy in the as-cast condition, M-F. The Brinell hardness for the M-F alloy at 20°C is determined as HB 90. Both heat-treated alloys R-T6 and M-T6 show the same hardness value of HB 143.

Table 3 Ultimate tensile strength (UTS), yield strength (YS), and ultimate elongation (UE) for investigated alloys

Alloy code	at 20°C			at 300°C		
	YS, MPa	UTS, MPa	UE, %	YS, MPa	UTS, MPa	UE, %
M-F	132	208	1.0	99	110	5.6
R-T6	350	358	0.3	136	149	2.9
M-T6	341	363	0.8	138	143	4.8

The results of fulfilled tests for P-refined alloy are shown in Fig. 3. In spite of the fact that specimens tested at the higher loading frequency had a higher number of cycles to failure, values of time to rupture were found to be close, especially for the case of 300°C.

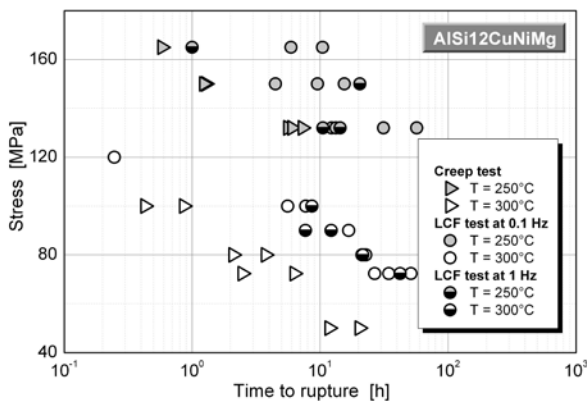


Fig. 3 Dependence of time to rupture vs. applied maximum stress for R-T6-alloy

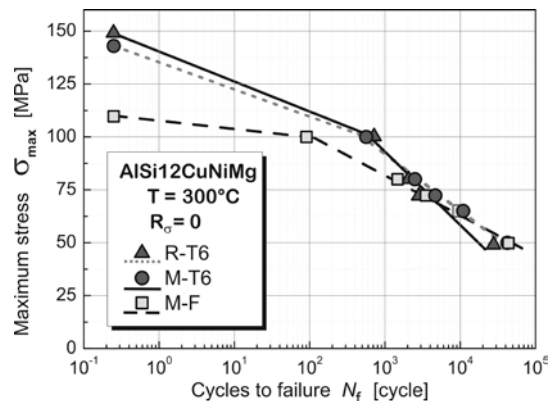


Fig. 4 Relationship between applied maximum stress and fatigue life of cycles to failure for investigated alloy conditions at 300°C

The averages of fatigue lives obtained for each maximum stress value in cyclic loading test at frequency of 0.1Hz are straight line fitted in Fig. 4. The experimental points on the far left correspond to creep strength values.

3. DISCUSSION

All investigated alloys show cyclic creep deformation response during low cycle fatigue tests under applied stresses. The comparison of ratcheting rate values shows that the M-F alloy accumulates permanent deformation during cyclic loading more rapidly than the heat-treated alloys. As a result, the Sr-modified alloy M-F has the lowest strength at low cycle fatigue loading at applied maximum stress higher than 65 MPa. This result is consistent with the observation [3] that Al-Si alloys with higher matrix hardness show better thermal fatigue resistance when compared to the Al-Si alloys without heat treatment. Under applied maximum stress lower than 65 MPa, similar values of fatigue lives for modified M-F and M-T6 alloys are expected. This can be explained by deterioration of mechanical properties in the M-T6 alloy due to overageing.

To establish the fracture mode, several ruptured specimens are observed with the help of optical and scanning electron microscopy. Primary silicon particles in the refined alloy R-T6 have a detrimental influence on fatigue behaviour. Cracking was often observed, particularly in large particles with a higher aspect ratio. The silicon particles appear to be sites for crack nucleation and propagation during loading. The decohesion and cracking of silicon particles at the fracture surface (see Fig. 5) reveal that these particles contribute to increasing the propagation rate of fatigue cracks and to shortening the fatigue life. The fracture process also includes the coalescence of voids and dimples in the matrix around those broken hard particles. For all R-T6 specimens, the fracture morphology consists of cleavage fracture of brittle-phase precipitates and cellular ductile fracture of the aluminum matrix with a high density of microdimples.

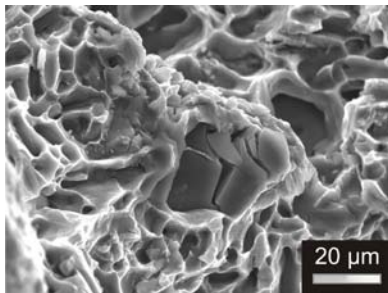


Fig. 5 SEM image of cracked silicon on a fracture surface of the specimen, R-T6

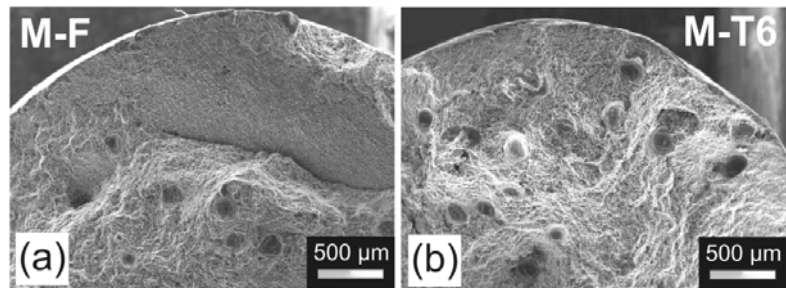


Fig. 6 SEM image of fracture surfaces after LCF testing with a maximum stress of 72 MPa: (a) M-F alloy and (b) M-T6 alloy

The observation of fracture surfaces of Sr-modified specimens in as-cast condition M-F and after heat treatment M-T6 leads to the conclusion that the porosity is the key factor affecting the fatigue strength in these alloys. No significant differences of fracture surfaces of modified alloy specimens between as-cast state M-F and the heat-treated state M-T6 are found (Fig.6). After observation of the fracture profile of M-T6 alloy specimens it is found that the main fracture path crosses the boundary zone eutectic/dendrites boundary of the alloy and the regions with pores.

Our results show that the Sr-modified and heat-treated alloy M-T6 displays slightly longer fatigue life compared to the refined alloy after T6 tempering R-T6 for applied maximum stress higher than 65 MPa in spite of the fact that the tested specimens of alloy M-T6 have casting imperfection of the gas porosity type. One may assume that the coarse and irregular morphology of silicon in the refined structure provides convenient paths for the crack to debond or cut through relatively easily, while the perfect spheroidizing of the eutectic silicon exerts more resistance to crack nucleation and crack growth.

4. MODELLING

It is known that deformation of metals at elevated temperature is rate-dependent process. In this case the unified theory of viscoplasticity may be applied [4]. We can start from a simple constitutive equation in the form of $\dot{\epsilon}_{in} = f_{\sigma}(\sigma_{eq})f_T(T)$.

Three functions of stress are applied to characterize minimum creep rate of R-T6 alloy [5]

$$\dot{\epsilon}_{\min} = A\sigma^n, \quad (1)$$

$$\dot{\epsilon}_{\min} = A \sinh(B\sigma), \quad (2)$$

$$\dot{\epsilon}_{\min} = A \frac{\sigma}{B} \left[1 + \left(\frac{\sigma}{B} \right)^{n-1} \right] \quad (3)$$

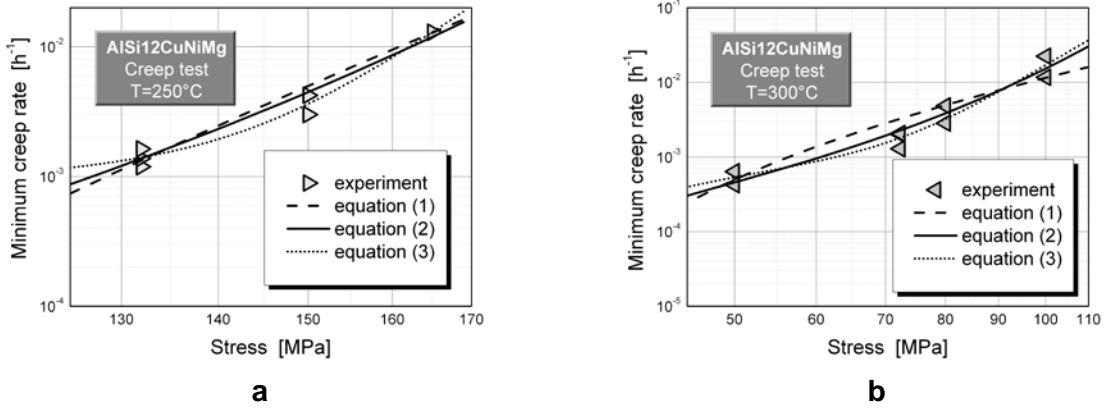


Fig. 7 Minimum creep rate vs. stress for R-T6 alloy at 250°C(a) and 300°C(b)

Figure 7 show that the hyperbolic sine law (2) describes the creep test results quite well. Introducing the function of stress (2) to be hyperbolic sine law, we can rewrite for uniaxial case

$$\dot{\epsilon}_{in} = A \sinh[B(\sigma - X)] \operatorname{sgn}(\sigma - X), \quad (4)$$

where X is the back stress, A and B are constants.

Evolution law of the back stress can be defined as non-linear kinematic hardening law

$$\dot{X} = C\dot{\epsilon}_{in} - D|\dot{\epsilon}_{in}|X \quad (5)$$

Equations (4) and (5) give possibility to simulate the primary and stationary stages of creep, as well as the strain ratcheting during cyclic loading with nonzero mean stress. The material constants were determined from results of tensile and creep tests. The verification of the model was done by comparison the calculated minimum ratcheting rate with values determined from tensile peak strain versus time experimental plots of R-T6 alloy (fig. 8).

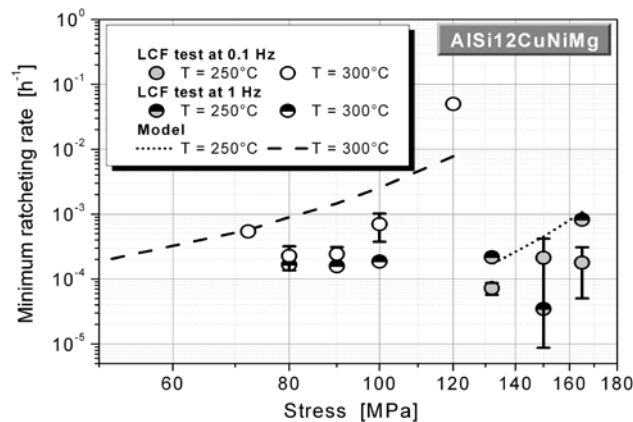


Fig. 8 Minimum ratcheting rate vs. stress for R-T6 alloy tested at temperature of 300°C.

The proposed model predicts the minimum ratcheting rate values good. To take into account tertiary creep, damage variables and damage evolution equations have to be included into proposed unified model.

CONCLUSION

Based on results from this study, we may conclude as follows:

1. Brittle fracture and decohesion of primary silicon particles together with the void growth and coalescence in the matrix are found to be the major factors affecting failure behavior of P-refined AlSi12CuNiMg alloy in the T6 condition.
2. Gas porosity is the main factor affecting the low cycle fatigue life of Sr-modified AlSi12CuNiMg alloy at elevated temperature.
3. The LCF behavior of P-refined and Sr-modified AlSi12CuNiMg alloys can be significantly improved by T6 heat treatment.
4. Under applied maximum stress lower than 65 MPa the number of cycles to failure for Sr-modified AlSi12CuNiMg alloy in both the as-cast and the T6 conditions is nearly similar due to deleterious effect of overageing of the heat-treated alloy during fatigue testing at temperature of 300°C.
5. The proposed simple unified model can well predict the material response under applied static and cyclic loading. To simulate the tertiary creep, damage variable will be introduced.

REFERENCES

- [1] Moreira M.F., Fuoco R. Characteristics of Fatigue Fractures in Al-Si Cast Components *AFS Trans.* Paper 06-122, pp. 1-15, 2006.
- [2] Silva F.S. Fatigue on engine pistons – A compendium of case studies *Eng. Failure Anal.*, Vol. 13, pp. 480-492, 2006.
- [3] Firouzdar V., Rajabi M., Nejati E., Khomamizadeh F. Effect of microstructural constituents on the thermal fatigue life of A319 aluminum alloy, *Mater. Sci. Eng.*, Vol. A 454-455, pp. 528-535, 2007.
- [4] Chaboche J.L. A review of some plasticity and viscoplasticity constitutive theories *Int. J. Plasticity*, Vol. 24, pp. 1642–1693, 2008.
- [5] Naumenko K., Altenbach H. *Modeling of creep for structural analysis*, Springer, 2007.